Science of the Total Environment 913 (2024) 169773

Contents lists available at ScienceDirect

Science of the Total Environment

journal homepage: www.elsevier.com/locate/scitotenv

Association between sea-land breeze and particulate matter in five coastal urban locations in India

V. Varaprasad, V.P. Kanawade *, A.C. Narayana *

Centre for Earth, Ocean and Atmospheric Sciences, University of Hyderabad, Hyderabad 500046, India

HIGHLIGHTS

- IGP pollution outflow onto the Bay of Bengal influences the eastern coast with reduced influence from north to south
- Sea-land breeze magnitude is negatively correlated with the particulate matter loading
- The weakened sea-land breeze would deteriorate air quality in coastal locations in a warming further climate

GRAPHICAL ABSTRACT

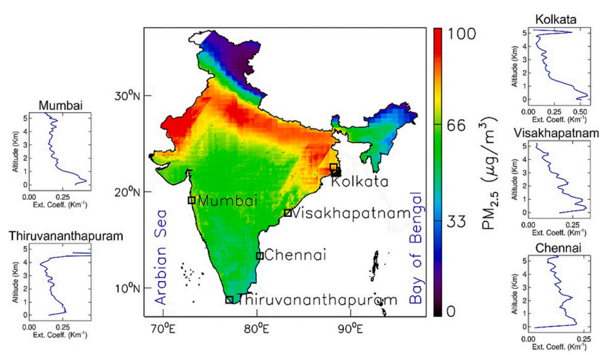

ARTICLE INFO

Guest Editor: Balram Ambade

Keywords:
Sea-land breeze system
Particulate matter
Coastal pollution
Air quality
Land-sea temperature contrast

ABSTRACT

Particulate matter less than 2.5 μm particle diameter ($PM_{2.5}$) is the most significant environmental issue globally. $PM_{2.5}$ is an integral component of air quality monitoring and management, human health, weather, climate, and epidemiological research. In this work, we investigate the seasonal variation in $PM_{2.5}$ mass concentrations and the association between the sea-land breeze system and particulate matter in five coastal urban locations in India (Kolkata, Visakhapatnam, Chennai, Thiruvananthapuram, and Mumbai). The relative occurrence of high $PM_{2.5}$ mass concentrations was the greatest during the winter season (December through February) while the relative occurrence of low $PM_{2.5}$ mass concentrations was the greatest during the monsoon season (June through September). Amongst locations, Kolkata experiences the highest $PM_{2.5}$ loading in winter while Thiruvananthapuram experiences the lowest $PM_{2.5}$ loading in monsoon. Indo-Gangetic Plain (IGP) outflow onto the Bay of Bengal significantly impacts locations along the eastern coast of India with reduced impact from north (Kolkata) to south (Chennai). The sea-breeze component analysis revealed daily cycles of the sea-land breeze with varying magnitudes of the breeze between the different seasons. Overall, we found a negative association between the sea-land breeze magnitude and $PM_{2.5}$ mass concentrations, implying that the weakened sea-land breeze may deteriorate air quality in coastal locations due to poor ventilation. The vertical profiles of aerosol extinction showed elevated aerosol layers within 1 km from the surface in almost all locations. The decreasing trend in the land-sea temperature contrast in coastal locations is expected to deteriorate air quality in coastal locations in the warming future. Nevertheless, critical analyses using ground-based remote sensing techniques are required for a better understanding the impact of sea-land breeze dynamics on air quality in coastal locations.

* Corresponding authors.
E-mail addresses: vijaykanawade03@yahoo.co.in (V.P. Kanawade), acnarayana@gmail.com (A.C. Narayana).

https://doi.org/10.1016/j.scitotenv.2023.169773
Received 15 May 2023; Received in revised form 13 November 2023; Accepted 28 December 2023
Available online 3 January 2024

1. Introduction

Air pollution is a transboundary problem and a subject of local-to-global scale concern. Industrialization and urbanization, which are an integral part of a country's economic and infrastructure development in rapidly developing countries such as India and China, bring in its wake several challenges like an increase in the population of urban settlements, an increase in industrialization and infrastructure, and increased vehicular movement, all of these cause increased near-surface pollution in the atmosphere (Martin et al., 2019). However, poor air quality in India is no longer an urban problem as semi-rural and/or rural areas also experience high pollution levels (Dey et al., 2020; Ravishankara et al., 2020). It is because air pollution over a region constitutes both the local emissions and advected pollution from distant sources (Cusworth et al., 2018; Ghude et al., 2011; Tan et al., 2022; Varaprasad et al., 2021). While in-cloud and below-cloud scavenging can remove 50–85 % of air pollutants (Grythe et al., 2017) thereby improving air quality, temperature inversion, shallow boundary layer height, low/calm wind speed, cold temperature, and high relative humidity along with high emission rates significantly deteriorates air quality (Chen et al., 2020b; Guttikunda and Gurjar, 2012; Kanawade et al., 2020; Mukherjee et al., 2018; Upadhyay et al., 2020). The study by Mishra et al. (2023) demonstrated the rapid nanoparticle growth driven by local and/or distant primary biomass burning emissions during nighttime leading to haze formation in Delhi. Thus, diverse pollution sources along with local micro-meteorology, regional atmospheric dynamics, and topography can worsen the air quality locally to regional scale. Human exposure to such deteriorated air pollution poses a serious health burden globally. About 670,000 deaths and 0.9 years of life expectancy loss were attributable to air pollution exposure in 2017 in India (Balakrishnan et al., 2019).

In India, numerous studies have used in-situ measurements, satellite data, reanalysis products and modelling approaches to examine spatio-temporal variability of continental air pollution (Gaur et al., 2014; Guttikunda et al., 2019; Martin et al., 2019; Police et al., 2016; Ravishankara et al., 2020; Singh et al., 2021; Srivastava et al., 2012; Tripathi et al., 2006; Vadrevu et al., 2020; Varaprasad et al., 2021), to investigate source-specific influence (biomass/agricultural burning, vehicular emissions, coal-fired power plants, etc.) (Cusworth et al., 2018; Ghude et al., 2008; Guttikunda and Jawahar, 2014; Kanawade et al., 2020; Mukherjee et al., 2018; Sahu et al., 2017), to study air pollution association with meteorological conditions and boundary layer dynamics (Budakoti and Singh, 2021; Guttikunda and Gurjar, 2012; Kanawade et al., 2020; Upadhyay et al., 2020), to study air pollution impacts on agriculture/vegetation (Agrawal et al., 2006; Agrawal et al., 2003; Burney and Ramanathan, 2014; Gupta et al., 2017) and human health (Balakrishnan et al., 2019; Chowdhury et al., 2018; Prabhakaran et al., 2020), and also to understand air pollution associated feedback from its interactions with climate (Burney and Ramanathan, 2014; Cramer, 2006; Kaur and Pandey, 2021; Ramanathan and Carmichael, 2008). However, air pollution studies in Indian coastal environments are sparse and limited to a few urban locations. For instance, Verma et al. (2016) showed an enhanced relative contribution of the aerosol layer to aerosol extinction at an altitude above 1 km due to the sea breeze activity over a coastal West Bengal and coal combustion was found to be the major source of air pollution in Kolkata (Gupta et al., 2007). Babu et al. (2016) have also found that bursts of ultrafine particles occur frequently during the sea-land breeze transition at Thiruvananthapuram. Source apportionment of aerosols study carried out by Police et al. (2016) revealed that biomass and coal burning are dominant sources of particulate matter in the coastal Visakhapatnam, while the other common pollutant sources are marine, the metal industry, and fuel combustion. Police et al. (2018) further examined the metal ion concentrations in coastal Mumbai and found that chlorine, magnesium, and sodium metal ion concentrations were the highest in the monsoon season, indicating the influence of natural marine aerosols. They further revealed that natural sources contribute the most to coarse mode particles while anthropogenic sources contribute significantly to the fine mode particles in coastal Mumbai. In coastal Chennai, EzhilKumar et al. (2021) have reported that sulphate is dominant, followed by sodium and calcium.

Additionally, the sea-land breeze system can contribute to poor air quality in urban coastal regions; firstly by back-and-forth air circulation within the sea-land breeze system (Li et al., 2020; Rimetz-Planchon et al., 2008), and secondly through the formation of the thermal internal boundary layer (TIBL) which inhibits the vertical dispersion of air pollutants (Comrie, 1988). Above the TIBL, the unmodified marine air acts as a cap that prevents mixing between destabilized marine air below and the continental air above (Stull, 1988). The presence of TIBL shown to be associated with increased surface-level particulate matter concentrations in a coastal city in North China (Wei et al., 2018). However, the number of threshold exceedance days and trends are relatively lower in coastal urban locations than in inland urban locations (Anand et al., 2019; Chen et al., 2020a; Gupta and Kumar, 2006; Singh et al., 2021). Recent studies showed the dominance of anthropogenic activities to $PM_{2.5}$ mass concentrations in coastal urban locations in India such as Mumbai, Thiruvananthapuram and Visakhapatnam (Police et al., 2016; Police et al., 2018; Sumesh et al., 2017). While the presence of a sea-land breeze may disperse pollutants to the sea, the diffused emissions are growing in coastal cities, Chennai and Visakhapatnam (Guttikunda et al., 2015). Williams et al. (2022) found an increase in aerosol loading with the dominance of coarser particles after the onset of sea breeze over a tropical semi-urban coastal location in India. The satellite-based study also showed the lofted aerosol layers above 1 km associated with the sea breeze activity over western coastal West Bengal (Verma et al., 2016).

The dynamical influence of sea-land breeze system on air pollution in coastal locations in India is poorly understood, except a study by Babu and Moorthy (2002) showing the increased dilution of near-surface black carbon aerosols by the reversal of surface winds over a tropical semi-urban coastal location, Thiruvananthapuram. Here we made an attempt to investigate the association between the sea-land breeze and particulate pollution in five coastal urban locations namely Kolkata, Visakhapatnam, Chennai, Thiruvananthapuram, and Mumbai. Kolkata, Visakhapatnam, and Chennai are located on the eastern coast of India while Thiruvananthapuram and Mumbai are located on the western coast of India. The western coastal plain has a narrow margin interspersed by mountainous terrain (tropical wet climate) while the eastern coastal plain is wide with well-developed deltas (tropical wet and dry climate). The eastern coast is strongly influenced by the Indo-Gangetic Plain (IGP) outflow of anthropogenic pollution onto the Bay of Bengal while the western coast is affected by the long-range transport of continental pollution.

2. Methods

2.1. Data locations

Fig. 1 shows the geographical location of five coastal urban locations in India. The filled contours indicate the averaged spatial distribution of ambient $PM_{2.5}$ from a satellite-based high-resolution (1 km) database (Dey et al., 2020). The details of population, surface elevation, sources of pollution, and geographical location of the Continuous Ambient Air Quality Monitoring Station (CAAQMS) for the five coastal urban cities are given in Table S1.

2.2. Data sources

$PM_{2.5}$ mass concentrations and meteorological data are obtained from the Central Pollution Control Board continuous ambient air quality monitoring station (CAAQMS) with a time resolution of 15 min (https://app.cpcbccr.com/ccr/#/caaqm-dashboard-all/caaqm-landing) for the time period from January 2016 to September 2022. The fifth-generation ECMWF reanalysis dataset (ERA5) provides hourly estimates of atmospheric, land, and oceanic climate variables. The data

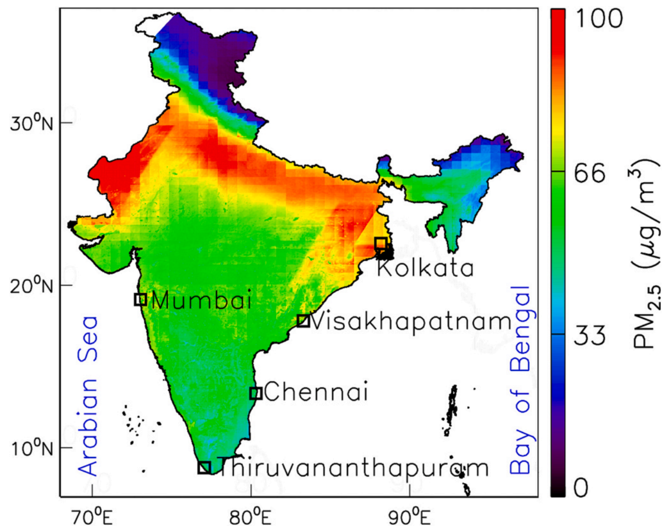

Fig. 1. Spatial distribution of satellite-derived high-resolution (1 km) ambient $PM_{2.5}$ concentrations adopted from "satellite-based application for air quality monitoring and management at a national scale" (SAANS) database, averaged over 2016–2019. Open square boxes denote the location of five urban coastal cities, namely Kolkata, Visakhapatnam, Chennai, Thiruvananthapuram, and Mumbai.

products cover the Earth on a 30 km grid spatial resolution and resolve the atmosphere vertically using 137 pressure levels from the surface to an altitude of 80 km (https://www.ecmwf.int/en/forecasts/dataset/ecmwf-reanalysis-v5). The ERA5 data is sufficiently reliable on offshore and flat onshore locations (Gualtieri, 2022). The boundary layer height, wind speed, and wind direction at the 10-m height at pressure levels from 1000 hPa to 500 hPa from ERA5 for the same time period are used here. The Cloud-Aerosol Lidar and Infrared Pathfinder Satellite Observations (CALIPSO) retrieved vertical profiles of the aerosol extinction coefficient are also used. The Level 2 Version 4.2 aerosol extinction coefficient at 532 nm for both day and night is used in this study for the same time period (https://subset.larc.nasa.gov/calipso/). The CALIPSO satellite provides the aerosol extinction coefficient which is a measure of the total attenuation of light by the aerosol particles in the atmosphere. The vertical resolution of the aerosol profile data varies as a function of altitude. In the tropospheric region, between −0.5 km and 20 km, the aerosol profile products are reported at a resolution of 60 m vertically (https://asdc.larc.nasa.gov/documents/calipso/quality_summaries/CALIOP_L2ProfileProducts_3.01.pdf). The technical details about CALIPSO are available in Winker et al. (2009). The Global Data Assimilation System (GDAS) $1^{\circ} \times 1^{\circ}$ gridded datasets from the National Oceanic and Atmospheric Administration (NOAA) are also used to calculate air mass backward trajectories.

2.3. Data quality control

The $PM_{2.5}$ data is obtained from the respective CAAQM stations for each city as shown in Table S1. Here, we have removed exceptionally low (less than 2 percentiles based on all data points) and high (greater than 98 percentiles) values of $PM_{2.5}$ data. This resulted in available data frequency of 87.8 %, 74.6 %, 84.2 %, 68.9 %, and 64.6 % at Kolkata, Visakhapatnam, Chennai, Thiruvananthapuram, and Mumbai, respectively. Further, the hourly and daily averages are calculated only if at least 50 % and 70 % of valid data points are available for each hour (total of 4 data points) and day (96 data points), respectively. The quality checks for CALIPSO retrieved aerosol profiles are done based on the conditions that are provided in the CALIPSO quality statements (https://asdc.larc.nasa.gov/documents/calipso/quality_summaries/CALIOP_L2ProfileProducts_3.01.pdf).

2.4. Analysis techniques

Since the wind data from CAAQM stations is very sparse, we used fifth-generation ECMWF reanalysis (ERA5) simulated hourly wind data at 10 m height above the ground for all five locations (Hersbach et al., 2018). The sea breeze component (SBC) was computed by resolving the wind speed and wind direction into the horizontal wind component following the methodology given by KiranKumar et al. (2019);

$$SBC = WS^{*}\ SIN(\Phi - WD) \quad (1)$$

where SBC is the sea breeze component (the positive value indicates the sea breeze while the negative value indicates the land breeze), WS is the wind speed in m/s, Φ is the coastal angle (the highest meteorological angle at which the coastline exists) and WD is the wind direction in degrees.

In general, the winds flowing perpendicular to the coastline have greater magnitudes, while the winds flowing parallel to the coastline have calm to zero speed. For example, if we consider, at two different times, the winds are flowing parallel and perpendicular to the coastline at 225° and 135°, with a high speed of 8 m/s, the resultant angle becomes 0°and 90° and the trigonometric sine function of 0 and 90 is zero and one, respectively. The resultant SBC becomes zero for winds flowing parallel to the coastline and 8 m/s for winds flowing perpendicular to the coastline. In this way, the equation can differentiate between the land breeze and sea breeze and the strength of the breezes. The calculated coastal angles for Kolkata, Visakhapatnam, Chennai, Thiruvananthapuram, and Mumbai are 270°, 225°, 195°, 325° and 350°, respectively.

We also used the ERA5 vertically-resolved wind data to investigate the vertical wind circulation and specific humidity in each location. The u, v, and w components of the wind at pressure levels from 1000 hPa to 500 hPa are used. First, the vertical velocity omega in Pa s^{-1} is converted into m/s (https://www.ncl.ucar.edu/Document/Functions/Contributed/omega_to_w.shtml), and then the u, v, and w streamlines function is plotted in metR package (Campitelli, 2021) in RSTUDIO software. The CALIPSO retrieved aerosol vertical profiles used to examine the vertical distribution of aerosols over the five locations. The obtained aerosol vertical profiles averaged for $1^{\circ} \times 1^{\circ}$ box over the CAAQMS location. The CALIPSO has an overpass over these locations from 1:30 PM to 3:30 PM local time during the day and 00:20 AM to 2:30 AM local time during the night. The NOAA's Hybrid Single Particle Lagrangian Integrated Trajectories (HYSPLIT) model was used to calculate 7-day hourly air mass backward trajectories starting at a height of 100 m above ground level from each location, using the GDAS reanalysis datasets (Draxler, 1999; Stein et al., 2015). The calculated air mass trajectories were then used to obtain the trajectory density map by using Trajstat software (Wang et al., 2009). The error in trajectory calculations for travel distance is estimated to be anywhere from 15 to 30 % associated with the physical, computational, meteorological parameters and forecast errors (https://www.arl.noaa.gov/documents/workshop/NAQC2007/HTML_Docs/trajerro.html).

The seasonal analysis was performed for four seasons namely winter (December to February, DJF), pre-monsoon (March to May, MAM), monsoon (June to September, JJAS), and post-monsoon (October to November, ON) (IMD, 2010). First, we calculated the frequency of occurrence of $PM_{2.5}$ mass concentrations to understand seasonal variability in $PM_{2.5}$ in all five locations followed by seasonal variability in the SBC. In the absence of ground-based remote sensing (LIDAR or Boundary layer RADAR) observations, the analyses intended to understand the sea-land breeze system influence on local to regional scale air pollution using a combination of ERA5 wind and CALIPSO retrieved aerosol vertical profile products.

3. Results

3.1. Frequency of occurrence and seasonal variation of $PM_{2.5}$

We used 24-h averaged mass concentrations of $PM_{2.5}$ to determine the seasonal relative occurrence frequency of $PM_{2.5}$ mass concentrations in five coastal urban locations (Fig. 2). The relative occurrence was computed as the ratio of the number of observations in a given season to the total number of observations. The relative occurrence frequency of high $PM_{2.5}$ mass concentrations was the greatest in the winter season (DJF) and the relative occurrence frequency of low $PM_{2.5}$ mass concentrations was the greatest in the monsoon season (JJAS). The maximum relative occurrence frequency of $PM_{2.5}$ mass concentrations was the highest and above the National Ambient Air Quality Standards (NAAQS, shown by red dashed line) in Kolkata and Visakhapatnam during post-monsoon (ON) and winter (DJF). In other locations (Chennai, Thiruvananthapuram, and Mumbai), $PM_{2.5}$ mass concentrations were also the highest during post-monsoon (ON) and winter (DJF) seasons, but $PM_{2.5}$ mass concentrations were lower than that of the 24-hour averaged NAAQS limit. This indicates that the quality of air in Kolkata and Visakhapatnam is severe to worst in the winter season as compared to other urban coastal locations.

About 60 % of the $PM_{2.5}$ mass concentration data points fall below the 24-hour NAAQS value of $PM_{2.5}$ (60 μg/m^3) while only 12 %, 1.7 %, 6 %, 23 %, and 9 % of the $PM_{2.5}$ mass concentration data points fall below the 24-hour average WHO standard value (15 μg/m^3) in Kolkata, Visakhapatnam, Chennai, Thiruvananthapuram, and Mumbai, respectively (Fig. 2). This is because the background $PM_{2.5}$ mass concentrations in India are very high and limiting it to WHO standard value will be very ambitious. Overall Kolkata has the lowest percentage (63 %) of days with $PM_{2.5}$ concentrations lower than the NAAQS value while Thiruvananthapuram has the highest percentage (~98 %) of days with $PM_{2.5}$ concentrations lower than the NAAQS value. Kolkata, Visakhapatnam, and Mumbai have less than 60 % of days $PM_{2.5}$ concentrations below the NAAQS limit during winter as compared to Chennai and Thiruvananthapuram.

We have further examined the seasonal variability in $PM_{2.5}$ mass concentrations in all five coastal urban locations (Fig. S1). $PM_{2.5}$ mass concentrations show strong seasonal variation in all coastal locations, with the highest $PM_{2.5}$ concentrations in the winter (DJF) and post-monsoon (ON) seasons and the lowest in the monsoon (JJAS) season. The observed seasonal variability in $PM_{2.5}$ mass concentrations can be explained by a combination of source (primary emission/second formation) and removal (dry/wet scavenging) rate of particulate matter, and planetary boundary layer evolution (dilution). The monthly average rainfall at each coastal urban location is shown in Fig. S2. Visakhapatnam and Chennai receive significant amounts of rainfall from November through January. The lowest mass concentrations of $PM_{2.5}$ in all locations during the monsoon (JJAS) season indicate efficient wet scavenging of particulate pollution while the highest mass concentrations in all locations during the winter (DJF) season indicate near-surface accumulation of particulate pollution owing to shallow boundary layer height, temperature inversion, less ventilation, and possibly higher emission source strength. Amongst locations, Kolkata experienced the highest $PM_{2.5}$ mass concentrations in winter (mean and standard deviation of 108 ± 49 μg/m^3) as compared to other locations. Overall, the sites located on the eastern coast of India have higher $PM_{2.5}$ mass concentrations (mean 48 μg/m^3) as compared to the western coast of India (32 μg/m^3). Previous studies demonstrated that the IGP pollution outflow onto the Bay of Bengal during winter (DJF) and pre-monsoon (MAM) seasons (Babu et al., 2012; Nair et al., 2013; Satheesh et al., 2006; Thomas et al., 2021) while the Arabian sea experiences inflow from arid/semi-arid African and Asian continents during pre-monsoon (MAM) (Aswini et al., 2020; Kumar et al., 2012). The outflow of IGP pollution onto the Bay of Bengal influences the atmospheric composition and radiation balance over the Bay of Bengal, including south-eastern peninsular India (Dasari et al., 2019). Thomas et al. (2021) showed about a 10–25 % reduction in aerosol loading over the IGP during COVID-19 enforced lockdown resulting in a 20–25 % reduction in aerosol-induced radiative forcing over the IGP outflow region of the Bay of Bengal. This demonstrates the significant influence of IGP outflow onto the Bay of Bengal and coastal regions further south.

3.2. Analysis of sea breeze component (SBC)

Fig. 3 shows the seasonal diurnal variation of occurrence frequency and 25th, 50th (median) and 75th percentile values of the sea breeze component in five coastal urban locations. Kolkata experiences the dominant wind flow from land to sea during post-monsoon (ON) and winter (DJF) seasons while it experiences the dominant wind flow from

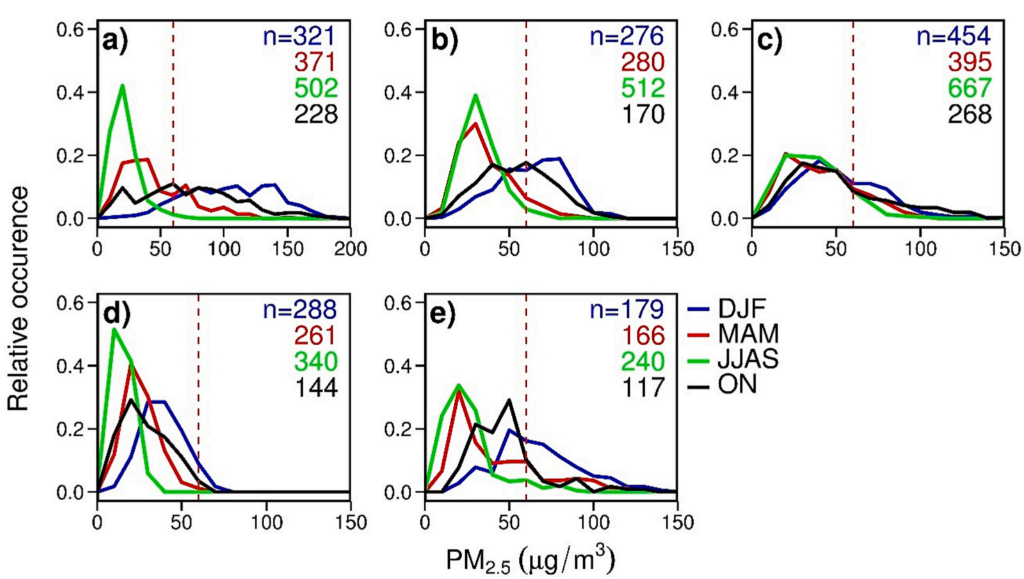

Fig. 2. Relative occurrence frequency of daily mean $PM_{2.5}$ mass concentrations in five coastal urban locations; a) Kolkata, b) Visakhapatnam, c) Chennai, d) Thiruvananthapuram, and e) Mumbai. 'n' indicates the total number of data points for each site during the four seasons (months) winter (DJF, blue), pre-monsoon (MAM, red), monsoon (JJAS, green) and post-monsoon (ON, black). The vertical red dashed line indicates NAAQS for the 24-hour average limit of $PM_{2.5}$ mass concentration (60 μg/m^3).

sea to land during pre-monsoon (MAM) and monsoon (JJAS) seasons. This corroborates the above finding of the higher relative occurrence of high $PM_{2.5}$ concentrations during post-monsoon (ON) and winter (DJF) seasons in Kolkata. The dominance of the nighttime land breeze during post-monsoon (ON) and winter (DJF) indicates the air pollution outflow onto the Bay of Bengal. Previous studies have also widely reported air pollution outflow onto the Bay of Bengal and the Arabian Sea (Aswini et al., 2020; Kumar et al., 2010; Thomas et al., 2019). The sea breeze is more intensified during pre-monsoon (MAM, high land-sea temperature contrast) and monsoon (JJAS, synoptic scale system such as Monsoon) which brings marine cleaner air masses to continental land. Overall, the diurnal pattern in SBC is obvious except in Kolkata, possibly because Kolkata is located away from the coastline (~ 100 km inland) and the inland penetration of the sea breeze depends upon the on-shore background winds. Overall, the sea breeze initiation varies from one season to another, with early initiation at about 8:00 AM local time in the pre-monsoon (MAM) season and late initiation at about 11:00 AM local time in the winter (DJF) season. Similarly, the land breeze initiation time also varies seasonally, with initiation time between 6:00 PM and 8:00 PM local time. We use collocated data points of SBC and $PM_{2.5}$ to further examine the association between the sea-land breeze and $PM_{2.5}$ and the results are presented in the following section.

The thick line denotes the median, the plus sign indicates the 25th and the asterisk indicates the 75th percentile.

3.3. Association between sea-land breeze and $PM_{2.5}$

To infer the association between $PM_{2.5}$ loading and the sea-land breeze (SBC), only the collocated valid data points were considered in the analysis. The analyses were performed separately for each season in five coastal urban locations. Fig. 4 shows contour plots of $PM_{2.5}$ loading versus SBC as a function of the occurrence frequency. The SBC greater than $SBC_{sea,75p}$ indicates the strengthened sea breeze, the SBC less than $SBC_{land,75p}$ indicates the strengthened land breeze, and the SBC between $SBC_{sea,75p}$ and $SBC_{land,75p}$ indicates weakened sea-land breeze. $PM_{2.5}$ greater than $PM_{2.5,75p}$ indicates a high PM loading. This implies that the occurrence frequency data points falling within the right top, middle, or bottom boxes is indicative of the high PM loading associated with the intensified sea, weakened, or intensified land breeze, respectively. Overall, the intensified sea-land breeze system in coastal locations appears to ventilate near-surface particulate pollution. The dominance of land breeze during post-monsoon (ON) and winter (DJF) and the sea

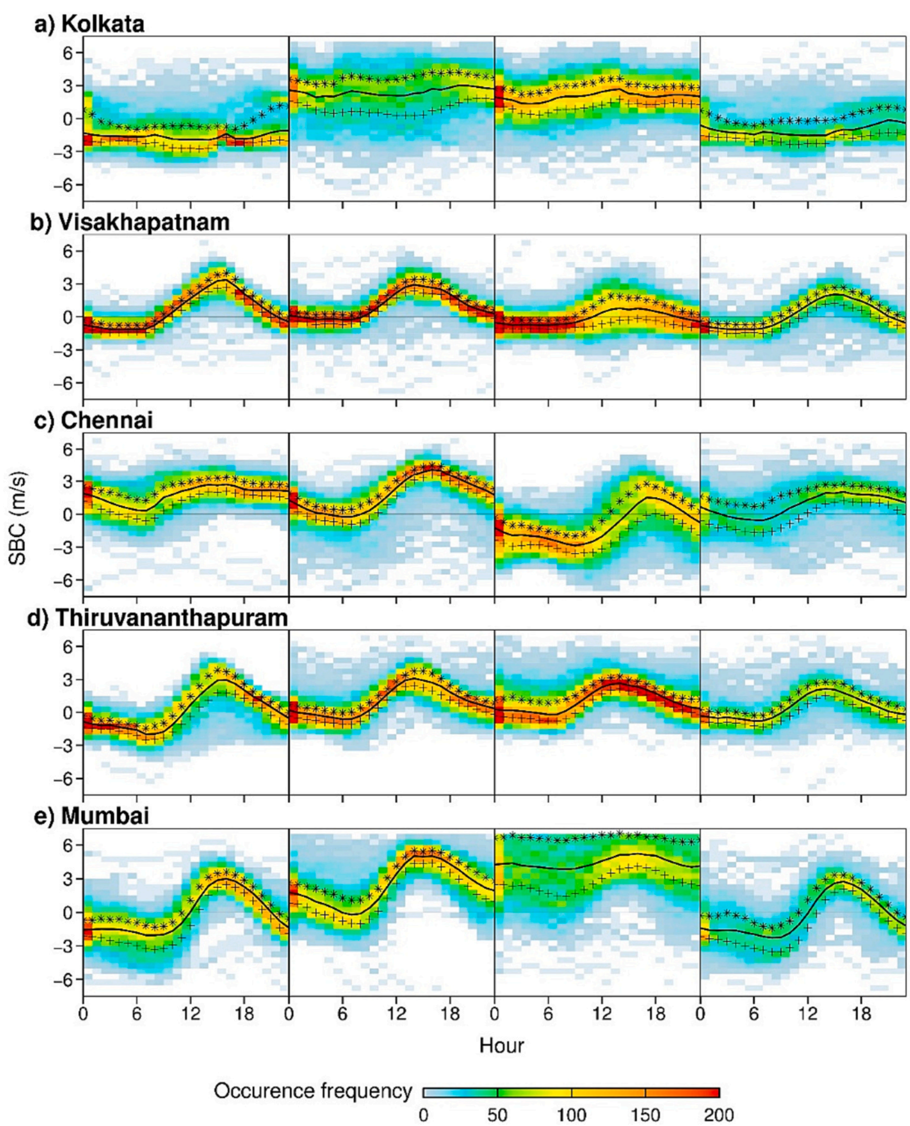

Fig. 3. Seasonal diurnal frequency of sea breeze component in five coastal urban locations; a) Kolkata, b) Visakhapatnam, c) Chennai, d) Thiruvananthapuram, and e) Mumbai. The positive values denote the sea breeze while the negative values denote the land breeze. The solid lines indicate the 25th, 50th (median), and 75th percentile values of the SBC.

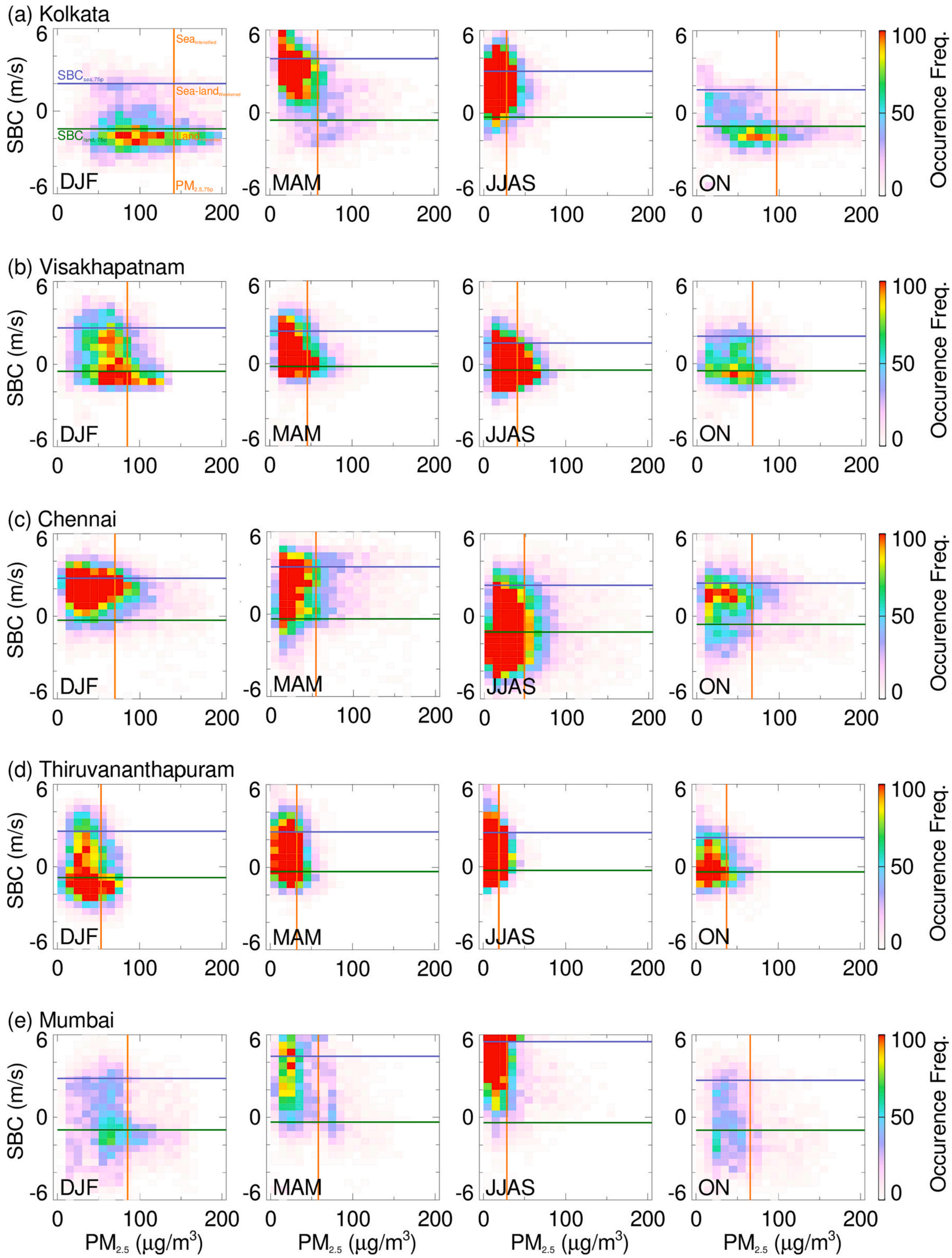

Fig. 4. Contour plot of $PM_{2.5}$ versus SBC as a function of the occurrence frequency for winter (DJF), pre-monsoon (MAM), Monsoon (JJAS) and post-monsoon (ON) seasons in five coastal urban locations; a) Kolkata, b) Visakhapatnam, c) Chennai, d) Thiruvananthapuram, and e) Mumbai. The horizontal blue line indicates the 75th percentile value of the sea breeze ($SBC_{sea,75p}$). The horizontal green line indicates the 75th percentile value of the land breeze ($SBC_{land,75p}$). The vertical orange line indicates the 75th percentile value of $PM_{2.5}$ ($PM_{2.5,75p}$). The right-side top, middle, and bottom regions indicate high PM loading associated with the strengthened sea breeze, weakened sea-land breeze, and strengthened land breeze, respectively.

breeze during pre-monsoon (MAM) and monsoon (JJAS) was observed in Kolkata (Fig. 4a). This is further corroborated by the HYSPLIT airmass backward trajectory analysis showing the prevalent northwest and southwest winds, respectively (Fig. S3a-d, first column). A similar association between $PM_{2.5}$ and SBC was observed in Visakhapatnam with reduced intensity of sea-land breeze (Figs. 4b, S3a-d, second column). This supports the earlier finding that the IGP pollution outflow onto the Bay of Bengal impact reduces further southward. In Chennai, the dominance of sea breeze was observed during post-monsoon (ON), winter (DJF), and pre-monsoon (MAM) seasons (Fig. 4c). The dominant land breeze during the monsoon (JJAS) was associated with monsoon synoptic wind flow structure. Thiruvananthapuram and Mumbai showed the relevant sea breeze during the pre-monsoon (MAM) and monsoon (JJAS) associated with the high sea-land temperature contrast and monsoon synoptic flow (Fig. S3), respectively.

To further examine the association between $PM_{2.5}$ and the sea-land breeze system, we have used collocated data points of $PM_{2.5}$ which were sorted as a function of SBC_{sea} and SBC_{land}. This way we have created two sets of collocated data samples (one for sea breeze and another for land breeze) for each location and season. Fig. S4 shows the binned scatter plot between $PM_{2.5}$ and SBC. Overall, a negative association between $PM_{2.5}$ and sea breeze (or land breeze) was observed for all seasons in all coastal locations. The observed negative associations are in agreement with the above finding (Fig. 4) showing the least occurrence frequency for high PM loading in all coastal locations. This further probably suggests that sea-land breeze dynamics had a less pronounced effect on air quality in these coastal locations. These results also highlight that the weakening of sea-land breeze speed may worsen the air quality in urban locations. To further examine the influence of sea-land breeze on the vertical distribution of particulate matter in coastal urban environments, we have used the CALIPSO retrieved vertical profiles of aerosol extinction and the collocated vertical wind structure from ERA5 which are discussed in the following section.

3.4. Vertical structure of aerosols and winds

Figs. 5 and 6 show the CALIPSO retrieved vertical profiles of the aerosol extinction coefficient and ERA5 planetary boundary layer height for daytime and nighttime, respectively. Overall, the elevated aerosol layers below 1 km were consistently observed in all coastal locations except in Visakhapatnam and Chennai during monsoon (JJAS) and post-monsoon (ON). There is no universal pattern but aerosol concentrations tend to decrease with increasing altitude in continental locations. In Kolkata, aerosol extinction peaks at about 300 m above the ground in winter (DJF), pre-monsoon (MAM) and post-monsoon (ON) seasons and at about 1 km in the monsoon (JJAS) season, with the highest near-surface aerosol extinction during winter (DJF) and with the lowest aerosol extinction in the monsoon (JJAS) season. The aerosol extinction has a twin peak within the planetary boundary height in the pre-monsoon (MAM). The elevated aerosol layers at altitudes of about 3 km and higher in coastal locations have also been reported in the literature (e.g. Verma et al., 2016) and have also been observed almost in all locations in this study which are not discussed here. In Visakhapatnam, a twin peak in aerosol extinction between the surface and 1 km altitude during winter (DJF) season was observed while other seasons did not show a prominent elevated aerosol layer within the planetary boundary layer. Aerosol extinction peak at about 300 m above the ground was also evident in Chennai, Thiruvananthapuram and Mumbai, particularly in winter (DJF) and pre-monsoon (MAM) seasons. Overall, the lowest near-surface aerosol extinction coefficient in Chennai and

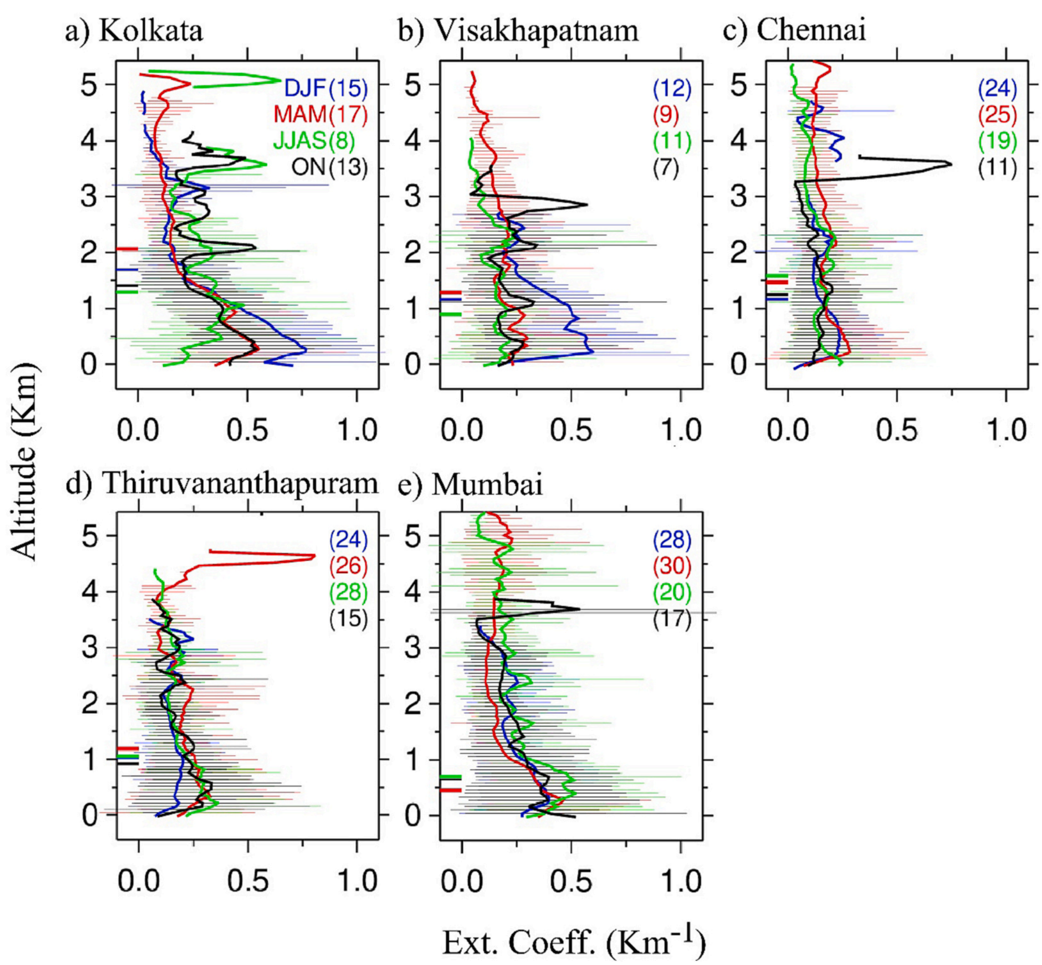

Fig. 5. CALIPSO retrieved daytime vertical profiles of aerosol extinction coefficient for five coastal urban locations; a) Kolkata, b) Visakhapatnam, c) Chennai, d) Thiruvananthapuram, and e) Mumbai during daytime. Colour indicates the seasons winter (DJF, blue), pre-monsoon (MAM, red), monsoon (JJAS, green), and post-monsoon (ON, black). The numbers in the brackets denote the number of vertical profiles available for the season. The error bars indicate the standard deviation of the aerosol extinction coefficient at each height. The planetary boundary layer height is shown by the horizontal coloured bar.

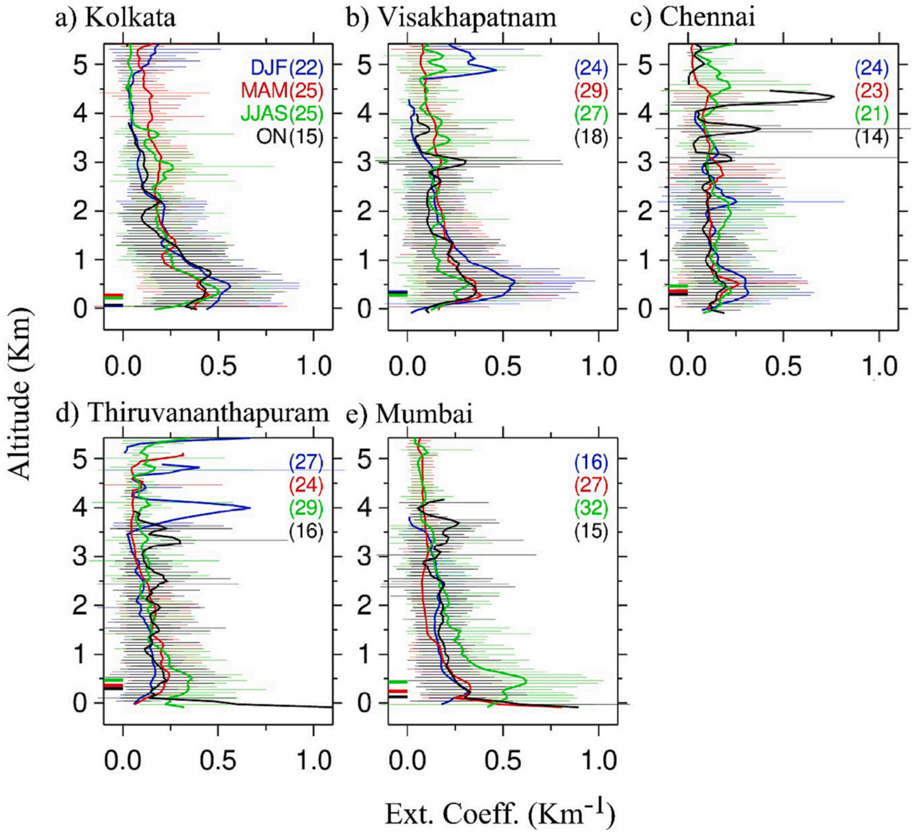

Fig. 6. Same as Fig. 5, but for nighttime.

Thiruvananthapuram is indicative of the low PM loading and/or lesser influence of long-range transported PM compared to that of in Mumbai, Kolkata or Visakhapatnam. Similar to daytime, vertically-resolved aerosol distribution can be observed during nighttime, with the elevated aerosol layers closer to the surface (300–500 m above the ground). Overall, the nighttime elevated aerosol layers are less pronounced than the daytime. Overall, the columnar aerosol concentrations are higher in urban coastal locations on the East Coast as compared to the urban coastal locations on the West Coast.

The air quality in a coastal city is affected by local sources, long-range transport, meteorological conditions and the sea-land breeze dynamics (Lam et al., 2005; Papanastasiou and Melas, 2009). We further examine the wind circulation patterns by applying the streamline analysis on vertical zonal wind velocity. Figs. 7 and 8 show the latitude/longitude-pressure cross-section of wind circulation and specific humidity in all urban coastal locations and seasons for daytime and nighttime, respectively for collocated CALIPSO overpasses. We have also performed similar analyses based on entire data (Figs. S5 and S6) which showed analogous variations. Overall, specific humidity illustrates the development of a sea-land breeze system with a well-defined onshore flow of moisture-laden air within a shallow layer above the surface. The strong wind flow from land to sea during both daytime and nighttime in post-monsoon (ON) and winter (DJF) seasons is evident at Kolkata substantiating earlier findings (Figs. 4, S3) showing IGP pollution outflow onto the Bay of Bengal. The wind flow from sea to land during both daytime and nighttime in post-monsoon (ON) and winter (DJF) seasons at Visakhapatnam and Chennai further confirms that IGP pollution outflow onto the Bay of Bengal can impact locations further south along the east coast. Mumbai and Thiruvananthapuram are impacted by in-land continental pollution during the post-monsoon (ON) and winter (DJF) seasons. The earlier studies showed that a well-developed sea breeze structure extends horizontally up to 100 km on the sea and 80 km on the land with a vertical extent of 1 km (Fan et al., 2008; Rani et al., 2010). The advection of cool and moist air over warm land surfaces leads to modification of the vertical structure of the atmospheric boundary layer and limits the height of the vertical mixing in the thermal internal boundary layer (Augustin et al., 2020). Further, the intensity and the time of occurrences of breezes depend on the background prevailing winds, on or off-shore cloud development, and the synoptic weather systems like cyclones (Anurose et al., 2012; KiranKumar et al., 2019; Reddy et al., 2021). Thiruvananthapuram and Mumbai experience the dominant land breeze during the winter (DJF) season, while they experience the dominant sea breeze component during the pre-monsoon (MAM) and monsoon (JJAS) seasons.

4. Discussions

Globally, the coastal regions are regularly impacted by the sea-land breeze phenomena and are thought to affect the air quality in coastal locations (Bouchlaghem et al., 2007; Han et al., 2023; Marley et al., 2022; Papanastasiou and Melas, 2009; Rodríguez et al., 2008; Tsai et al., 2011; Verma et al., 2016; Wei et al., 2018; Xiao et al., 2023). Our analyses showed that the initiation time of sea (land) breeze vary from 8:00 am to 11:00 am local time (6:00 pm to 8:00 pm local time) seasonally, analogues to previous finding showing seasonality in the onset and cessation times of sea-land breeze (KiranKumar et al., 2019). Wei et al. (2018) showed that the particulate matter concentrations rapidly increased in Qinhuangdao, a coastal city in North China, when thermal internal boundary layer formed, leading to rapid accumulation of pollutants near the surface during evening and night compared to when no thermal internal boundary layer was present during night Our observation also showed sea-land breeze development with well-defined onshore flow of marine air and elevated aerosol layers within 1 km above the surface in coastal urban locations in India. A typical sea-land breeze episode can be extended ~50 km inland and 300 m vertically which can give rise to elevated aerosol layers onshore in coastal

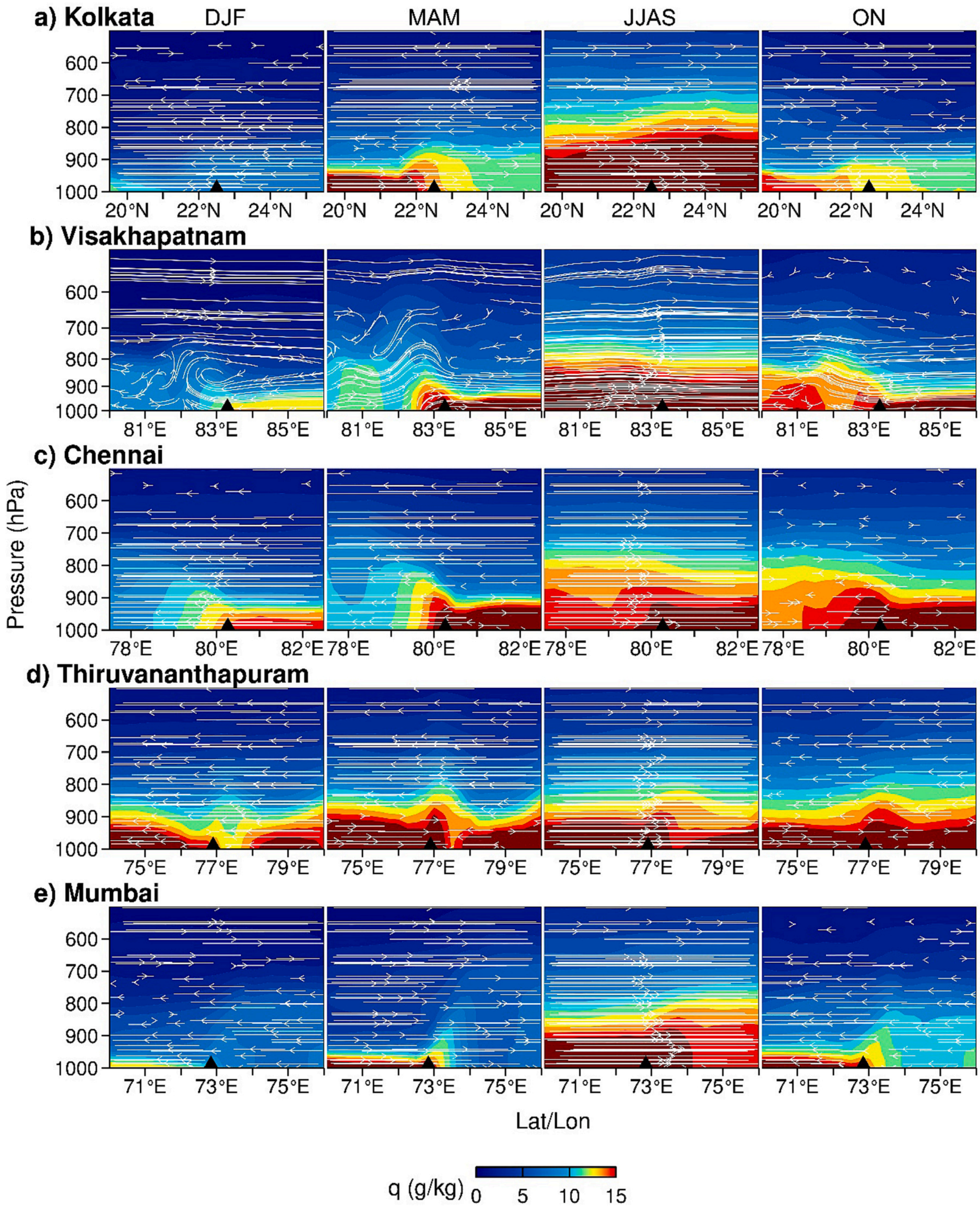

Fig. 7. Latitude/longitude-pressure cross-section of wind circulation (streamlines) and specific humidity (filled contour) during daytime in coastal urban locations; a) Kolkata, b) Visakhapatnam, c) Chennai, d) Thiruvananthapuram, and e) Mumbai during different seasons and collocated to CALIPSO measurements. The black triangle on the x-axis denotes the City location.

locations (Han et al., 2023), Using 15 years of observations from coastal, urban and marine locations, Xiao et al. (2023) showed the weakening of the sea-land breeze in Tianjin, a coastal megacity in China as a result of the reduced thermal contrast between sea and land driven by urbanization and ocean warming. Our analyses also showed that seas (the Arabian Sea and the Bay of Bengal) are warming at a faster rate than the adjoining land (Southern Peninsular), resulted in the reduced thermal contrast (Fig. 9). Thus, the urbanization of coastal cities in terms of infrastructure, land use and land cover change together with the projected ocean warming would weaken the sea-land breeze system and thus may result into weakened sea-land breeze. This would dampen back-and-forth circulation within the sea-land boundary layer structure and thus horizontal ventilation of air pollutants on/off shore in coastal environments, leading to the deterioration of air quality in coastal regions.

5. Conclusions

In this study, we used about seven years of $PM_{2.5}$ mass concentration data to investigate the seasonal variation in $PM_{2.5}$ mass concentrations

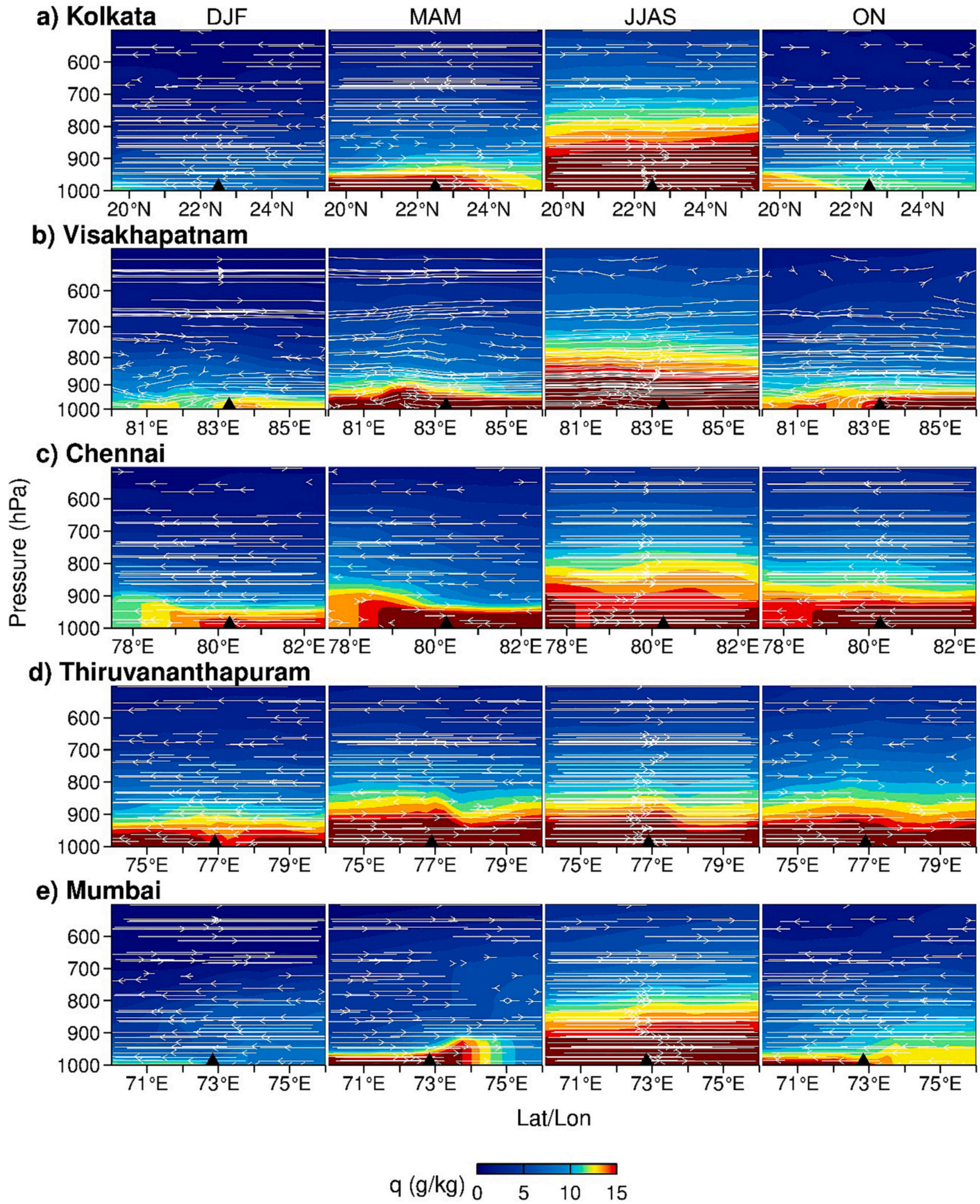

Fig. 8. Same as Fig. 7, but for nighttime.

and the association between the sea-land breeze and the particulate pollution in five coastal urban locations in India namely, Kolkata, Visakhapatnam, Chennai, Thiruvananthapuram, and Mumbai.

We found that Kolkata has the highest percentage of days exceeding the NAAQS limit of $PM_{2.5}$ concentrations and Thiruvananthapuram has the lowest percentage of days exceeding the NAAQS limit. Only a small fraction of days at all locations meet the WHO limit as the background $PM_{2.5}$ concentrations (natural and anthropogenic) are relatively high in India. Considering all locations, the highest $PM_{2.5}$ mass concentrations were observed in winter (DJF) while the lowest $PM_{2.5}$ mass concentrations were observed in monsoon (JJAS). The calculated sea-breeze component reveals the daily cycles of the sea-land breeze system in all coastal locations with varying magnitudes. The association between $PM_{2.5}$ and SBC as a function of the occurrence frequency reveals the features of the sea-land breeze system in these coastal locations. The negative association between $PM_{2.5}$ and SBC indicates that the weakening of the sea-land breeze system would deteriorate air quality in coastal locations due to poor ventilation. The presence of elevated aerosol layers within 1 km from the surface possibly indicates the accumulation of particulate matter under the influence of sea-land breeze system development which is illustrated by the well-defined onshore flow of marine air.

Overall, Indo-Gangetic Plain (IGP) outflow onto the Bay of Bengal impacts locations along the eastern coast of India with reduced impact from north (Kolkata) to south (Chennai) and the coastal locations on the east coast are more polluted than the locations on the west coast. Our analyses also highlight that the weakened sea-land breeze intensity under warming ocean and land scenario may deteriorate air quality in coastal region via reduced ventilation. Therefore, dedicated measurements using ground-based remote sensing techniques for atmospheric

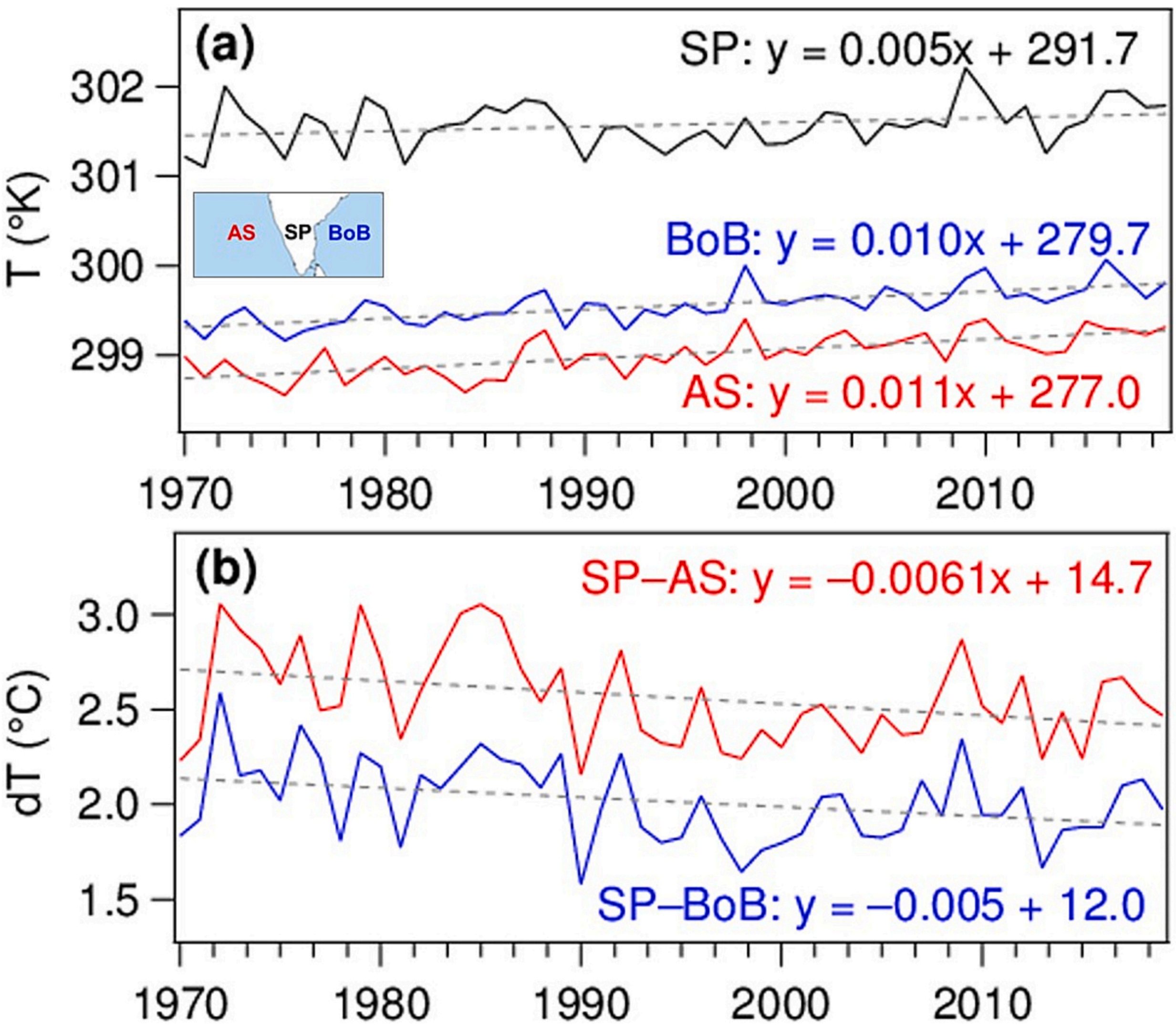

Fig. 9. (a) Trend in the averaged air temperature for lower tropospheric column (1000 hPa to 700 hPa) over the Arabian Sea (AS), the Southern Peninsular (SP) and the Bay of Bengal (BoB) and (b) trend in the land-sea temperature contrast.

pollutants and dynamics are required for a better understanding of the association between the sea-land breeze and air quality in coastal locations.

CRediT authorship contribution statement

VPK and ACN conceptualized and designed the idea. VV and VPK performed data analysis and interpretation. VV wrote the first draft. All authors contributed to the editing of the manuscript.

Declaration of competing interest

The authors declare that they have no known competing personal or financial relationships that could have appeared to influence the work reported in this paper.

Data availability

$PM_{2.5}$ gridded mass concentrations are available to download from http://www.saans.co.in/home.html and refer to Dey et al. (2020) for more details.

In-situ measurements of $PM_{2.5}$ are available to download from the Central Pollution Control Board website - https://airquality.cpcb.gov.in/ccr/#/caaqm-dashboard-all/caaqm-landing (Accessed on 25 Nov. 2022).

Wind and specific humidity datasets were obtained from Copernicus Climate Change Service, Climate Data Store, (2023): ERA5 hourly data on single levels and pressure levels from 1940 to present. (https://cds.climate.copernicus.eu/cdsapp#!/dataset/reanalysis-era5-pressure-levels?tab=overview) (Accessed on 25 Nov. 2022).

CALIPSO aerosol extinction vertical profiles were obtained from the NASA Langley Research Centre Atmospheric Science Data Centre at https://subset.larc.nasa.gov/calipso/ (Accessed on 25 Nov. 2022).

Acknowledgements

The authors would like to thank Central Pollution Control Board for free access to particulate matter and meteorological data. VV would like to acknowledge SRF from the University Grants Commission, New Delhi. Fifth generation of ECMWF atmospheric reanalyses of the global climate (ERA5) data were obtained from Copernicus Climate Change Service Climate Data store (CDS) at https://cds.climate.copernicus.eu/cdsapp#!/home. The CALIOP Level 2 V4.20 data were obtained from the NASA Langley Research Centre Atmospheric Science Data Centre at https://asdc.larc.nasa.gov/project/CALIPSO. The authors gratefully acknowledge the NOAA Air Resources Laboratory (ARL) for the provision of the HYSPLIT transport and dispersion model used in this publication. The authors acknowledge the use of Meteo-Info and Trajstat software. The authors also acknowledge the developers of the programming language R and RStudio Team (*http://www.rstudio.com/*). The authors are thankful to Chandan Sarangi and Roxy Koll for fruitful discussion. The authors are truly grateful to anonymous reviewers for their constructive suggestions to improve the novelty of the results presented in this publication.

Appendix A. Supplementary data

Supplementary data to this article can be found online at https://doi.org/10.1016/j.scitotenv.2023.169773.

References

Agrawal, M., Singh, B., Rajput, M., Marshall, F., Bell, J.N., 2003. Effect of air pollution on peri-urban agriculture: a case study. Environ. Pollut. 126 (3), 323–329.

Agrawal, M., Singh, B., Agrawal, S.B., Bell, J.N.B., Marshall, F., 2006. The effect of air pollution on yield and quality of mung bean grown in peri-urban areas of Varanasi. Water Air Soil Pollut. 169, 239–254.

Anurose, T.J., Subrahamanyam, D.B., Dutt, C.B.S., Kumar, N.V.P.K., John, S.R., Nair, S. K., Santosh, M., Mohan, M., Kunhikrishnan, P.K., Sijikumar, S., Prijith, S.S., 2012. Vertical structure of sea-breeze circulation over Thumba (8.5°N, 76.9°E, India) in the winter months and a case study during W-ICARB field experiment. Meteorog. Atmos. Phys. 115, 113–121.

Anand, V., Korhale, N., Rathod, A., Beig, G., 2019. On processes controlling fine particulate matters in four Indian megacities. Environ. Pollut. 254, 113026.

Aswini, A.R., Hegde, P., Aryasree, S., Girach, I.A., Nair, P.R., 2020. Continental outflow of anthropogenic aerosols over Arabian Sea and Indian Ocean during wintertime: ICARB-2018 campaign. Sci. Total Environ. 712, 135214.

Augustin, P., Billet, S., Crumeyrolle, S., Deboudt, K., Dieudonné, E., Flament, P., Fourmentin, M., Guilbaud, S., Hanoune, B., Landkocz, Y., Méausoone, C., Roy, S., Schmitt, F.G., Sentchev, A., Sokolov, A., 2020. Impact of sea breeze dynamics on atmospheric pollutants and their toxicity in industrial and urban coastal environments. Remote Sens. 12, 4.

Babu, S.S., Moorthy, K.K., 2002. Aerosol black carbon over a tropical coastal station in India. Geophys. Res. Lett. 29, 23, 13-1-13-14.

Babu, S.S., Gogoi, M.M., Kumar, V.H.A., Nair, V.S., Moorthy, K.K., 2012. Radiative properties of Bay of Bengal aerosols: spatial distinctiveness and source impacts. J. Geophys. Res. Atmos. 117, D6.

Babu, S.S., Kompalli, S.K., Moorthy, K.K., 2016. Aerosol number size distributions over a coastal semi urban location: seasonal changes and ultrafine particle bursts. Sci. Total Environ. 563-564, 351–365.

Balakrishnan, K., Dey, S., Gupta, T., Dhaliwal, R.S., Brauer, M., Cohen, A.J., Stanaway, J. D., Beig, G., Joshi, T.K., Aggarwal, A.N., Sabde, Y., Sadhu, H., Frostad, J., Causey, K., Godwin, W., Shukla, D.K., Kumar, G.A., Varghese, C.M., Muraleedharan, P., Agrawal, A., Anjana, R.M., Bhansali, A., Bhardwaj, D., Burkart, K., Cercy, K., Chakma, J.K., Chowdhury, S., Christopher, D.J., Dutta, E., Furtado, M., Ghosh, S., Ghoshal, A.G., Glenn, S.D., Guleria, R., Gupta, R., Jeemon, P., Kant, R., Kant, S., Kaur, T., Koul, P.A., Krish, V., Krishna, B., Larson, S.L., Madhipatla, K., Mahesh, P.A., Mohan, V., Mukhopadhyay, S., Mutreja, P., Naik, N., Nair, S., Nguyen, G., Odell, C. M., Pandian, J.D., Prabhakaran, D., Prabhakaran, P., Roy, A., Salvi, S., Sambandam, S., Saraf, D., Sharma, M., Shrivastava, A., Singh, V., Tandon, N., Thomas, N.J., Torre, A., Xavier, D., Yadav, G., Singh, S., Shekhar, C., Vos, T., Dandona, R., Reddy, K.S., Lim, S.S., Murray, C.J.L., Venkatesh, S., Dandona, L., 2019. The impact of air pollution on deaths, disease burden, and life expectancy across the states of India: the global burden of disease study 2017. Lancet Planet. Health 3 (1), E26–E39.

Bouchlaghem, K., Mansour, F.B., Elouragini, S., 2007. Impact of a sea breeze event on air pollution at the Eastern Tunisian Coast. Atmos. Res. 86 (2), 162–172.

Budakoti, S., Singh, C., 2021. Examining the characteristics of planetary boundary layer height and its relationship with atmospheric parameters over Indian sub-continent. Atmos. Res. 264, 105854.

Burney, J., Ramanathan, V., 2014. Recent climate and air pollution impacts on Indian agriculture. Proc. Natl. Acad. Sci. 111 (46), 16319–16324.

Campitelli, E., 2021. metR: tools for easier analysis of meteorological fields.

Chen, Y., Wild, O., Conibear, L., Ran, L., He, J., Wang, L., Wang, Y., 2020a. Local characteristics of and exposure to fine particulate matter ($PM_{2.5}$) in four Indian megacities. Atmos. Environ. X 5, 100052.

Chen, Z., Chen, D., Zhao, C., Kwan, M.P., Cai, J., Zhuang, Y., Zhao, B., Wang, X., Chen, B., Yang, J., Li, R., He, B., Gao, B., Wang, K., Xu, B., 2020b. Influence of meteorological conditions on $PM_{2.5}$ concentrations across China: a review of methodology and mechanism. Environ. Int. 139, 105558.

Chowdhury, S., Dey, S., Smith, K.R., 2018. Ambient $PM_{2.5}$ exposure and expected premature mortality to 2100 in India under climate change scenarios. Nat. Commun. 9, 1,318.

Comrie, A.C., 1988. Growth, Structure and Prediction of the Thermal Internal Boundary Layer. University of Cape Town.

Cramer, W., 2006. Air pollution and climate change both reduce Indian rice harvests. Proc. Natl. Acad. Sci. 103 (52), 19609–19610.

Cusworth, D.H., Mickley, L.J., Sulprizio, M.P., Liu, T., Marlier, M.E., DeFries, R.S., Guttikunda, S.K., Gupta, P., 2018. Quantifying the influence of agricultural fires in Northwest India on urban air pollution in Delhi, India. Environ. Res. Lett. 13, 044018.

Dasari, S., Andersson, A., Bikkina, S., Holmstrand, H., Budhavant, K., Satheesh, S., Asmi, E., Kesti, J., Backman, J., Salam, A., Bisht, D.S., Tiwari, S., Hameed, Z., Gustafsson, Ö., 2019. Photochemical degradation affects the light absorption of water-soluble brown carbon in the South Asian outflow. Sci. Adv. 5, 1, eaau8066.

Dey, S., Purohit, B., Balyan, P., Dixit, K., Bali, K., Kumar, A., Imam, F., Chowdhury, S., Ganguly, D., Gargava, P., Shukla, V.K., 2020. A satellite-based high-resolution (1-km) ambient $PM_{2.5}$ database for India over two decades (2000–2019): applications for air quality management. Remote Sens. 12, 23, 3872.

Draxler, R.R., 1999. HYSPLIT4 user's Guide. NOAA Tech. Memo. ERL ARL-230,. NOAA Air Resources Laboratory, Silver Spring, MD.

EzhilKumar, M.R., Karthikeyan, S., Chianese, E., Tirimberio, G., Di Gilio, A., Palmisani, J., Miniero, V.D., Cotugno, P., Riccio, A., 2021. Vertical transport of $PM_{2.5}$ and PM_{10} and its source identification in the street canyons of Chennai metropolitan city, India. Atmos. Pollut. Res. 12, 1, 173–183.

Fan, S., Wang, B., Tesche, M., Engelmann, R., Althausen, A., Liu, J., Zhu, W., Fan, Q., Li, M., Ta, N., Song, L., Leong, K., 2008. Meteorological conditions and structures of atmospheric boundary layer in October 2004 over Pearl river delta area. Atmos. Environ. 42 (25), 6174–6186.

Gaur, A., Tripathi, S., Kanawade, V.P., Tare, V., Shukla, S.P., 2014. Four-year measurements of trace gases (SO_2, NO_x, CO, and O_3) at an urban location, Kanpur, in Northern India. J. Atmos. Chem. 71 (4), 283–301.

Ghude, S.D., Fadnavis, S., Beig, G., Polade, S.D., van Der, A.R.J., 2008. Detection of surface emission hot spots, trends, and seasonal cycle from satellite-retrieved NO_2 over India. J. Geophys. Res. Atmos. 113, D20.

Ghude, S.D., Beig, G., Kulkarni, P.S., Kanawade, V.P., Fadnavis, S., Remedios, J.J., Kulkarni, S.H., 2011. Regional CO pollution over the Indian-subcontinent and various transport pathways as observed by MOPITT. Int. J. Remote Sens. 32 (21), 6133–6148.

Grythe, H., Kristiansen, N.I., Groot Zwaaftink, C.D., Eckhardt, S., Ström, J., Tunved, P., Krejci, R., Stohl, A., 2017. A new aerosol wet removal scheme for the Lagrangian particle model FLEXPART v10. Geosci. Model Dev. 10, 1447–1466.

Gualtieri, G., 2022. Analysing the uncertainties of reanalysis data used for wind resource assessment: a critical review. Renew. Sust. Energ. Rev. 167, 112741.

Gupta, I., Kumar, R., 2006. Trends of particulate matter in four cities in India. Atmos. Environ. 40 (14), 2552–2566.

Gupta, A.K., Karar, K., Srivastava, A., 2007. Chemical mass balance source apportionment of PM_{10} and TSP in residential and industrial sites of an urban region of Kolkata, India. J. Hazard. Mater. 142 (1–2), 279–287.

Gupta, R., Somanathan, E., Dey, S., 2017. Global warming and local air pollution have reduced wheat yields in India. Clim. Chang. 140, 593–604.

Guttikunda, S.K., Gurjar, B.R., 2012. Role of meteorology in seasonality of air pollution in megacity Delhi, India. Environ. Monit. Assess. 184 (5), 3199–3211.

Guttikunda, S.K., Jawahar, P., 2014. Atmospheric emissions and pollution from the coal-fired thermal power plants in India. Atmos. Environ. 92, 449–460.

Guttikunda, S., Goel, R., Mohan, D., Tiwari, G., Gadepalli, R., 2015. Particulate and gaseous emissions in two coastal cities - Chennai and Vishakhapatnam, India. Air Qual. Atmos. Health 8 (6), 559–572.

Guttikunda, S.K., Nishadh, K.A., Jawahar, P., 2019. Air pollution knowledge assessments (APnA) for 20 Indian cities. Urban Clim. 27, 124–141.

Han, S., Hao, T., Yang, X., Yang, Y., Luo, Z., Zhang, Y., Tang, Y., Lu, M., 2023. Land-sea difference of the planetary boundary layer structure and its influence on $PM_{2.5}$ - observation and numerical simulation. Sci. Total Environ. 858, 159881.

Hersbach, H., Bell, B., Berrisford, P., Biavati, G., Horányi, A., Muñoz Sabater, J., Nicolas, J., Peubey, C., Radu, R., Rozum, I., Schepers, D., Simmons, A., Soci, C., Dee, D., Thépaut, J.-N., 2018. ERA5 hourly data on single levels from 1959 to present. Copernicus Climate Change Service (C3S) Climate Data Store (CDS).

IMD, 2010. Climate profile of India. In: Met Monograph No. Environment Meteorology-01/2010, by Indian Meteorological Department, New Delhi.

Kanawade, V.P., Srivastava, A.K., Ram, K., Asmi, E., Vakkari, V., Soni, V.K., Varaprasad, V., Sarangi, C., 2020. What caused severe air pollution episode of November 2016 in New Delhi? Atmos. Environ. 222, 117125.

Kaur, R., Pandey, P., 2021. Air pollution, climate change, and human health in Indian cities: a brief review. Front. Sustain. Cities 3.

KiranKumar, N.V.P., Jagadeesh, K., Niranjan, K., Rajeev, K., 2019. Seasonal variations of sea breeze and its effect on the spectral behaviour of surface layer winds in the coastal zone near Visakhapatnam, India. J. Atmos. Sol. Terr. Phys. 186, 1–7.

Kumar, A., Sarin, M.M., Srinivas, B., 2010. Aerosol iron solubility over Bay of Bengal: role of anthropogenic sources and chemical processing. Mar. Chem. 121 (1–4), 167–175.

Kumar, A., Sudheer, A.K., Goswami, V., Bhushan, R., 2012. Influence of continental outflow on aerosol chemical characteristics over the Arabian Sea during winter. Atmos. Environ. 50, 182–191.

Lam, K.S., Wang, T.J., Wu, C.L., Li, Y.S., 2005. Study on an ozone episode in hot season in Hong Kong and transboundary air pollution over Pearl River delta region of China. Atmos. Environ. 39 (11), 1967–1977.

Li, W., Wang, Y., Bernier, C., Estes, M., 2020. Identification of sea breeze recirculation and its effects on ozone in Houston, TX, during DISCOVER-AQ 2013. J. Geophys. Res. Atmos. 125, 22, e2020JD033165.

Marley, H.G., McKendry, I., Dirks, K.N., Salmond, J.A., 2022. The impact of land-sea breezes on the formation of brown haze in an urban isthmus environment. Atmos. Pollut. Res. 13 (9), 101519.
Martin, R.V., Brauer, M., van Donkelaar, A., Shaddick, G., Narain, U., Dey, S., 2019. No one knows which city has the highest concentration of fine particulate matter. Atmos. Environ.: X. 3, 100040.
Mishra, S., Tripathi, S.N., Kanawade, V.P., Haslett, S.L., Dada, L., Ciarelli, G., Kumar, V., Singh, A., Bhattu, D., Rastogi, N., Daellenbach, K.R., Ganguly, D., Gargava, P., Slowik, J.G., Kulmala, M., Mohr, C., El-Haddad, I., Prevot, A.S.H., 2023. Rapid night-time nanoparticle growth in Delhi driven by biomass-burning emissions. Nat. Geosci. 16, 224–230.
Mukherjee, T., Asutosh, A., Pandey, S.K., Yang, L., Gogoi, P.P., Panwar, A., Vinoj, V., 2018. Increasing potential for air pollution over megacity New Delhi: a study based on 2016 Diwali episode. Aerosol Air Qual. Res. 18 (9), 2510–2518.
Nair, V.S., Moorthy, K.K., Babu, S.S., 2013. Influence of continental outflow and ocean biogeochemistry on the distribution of fine and ultrafine particles in the marine atmospheric boundary layer over Arabian Sea and Bay of Bengal. J. Geophys. Res. Atmos. 118 (13), 7321–7331.
Papanastasiou, D.K., Melas, D., 2009. Climatology and impact on air quality of sea breeze in an urban coastal environment. Int. J. Climatol. 29 (2), 305–315.
Police, S., Sahu, S.K., Pandit, G.G., 2016. Chemical characterization of atmospheric particulate matter and their source apportionment at an emerging industrial coastal city, Visakhapatnam, India. Atmos. Pollut. Res. 7 (4), 725–733.
Police, S., Sahu, S.K., Tiwari, M., Pandit, G.G., 2018. Chemical composition and source apportionment of $PM_{2.5}$ and $PM_{2.5–10}$ in Trombay (Mumbai, India), a coastal industrial area. Particuology 37, 143–153.
Prabhakaran, D., Mandal, S., Krishna, B., Magsumbol, M., Singh, K., Tandon, N., Narayan, K.M.V., Shivashankar, R., Kondal, D., Ali, M.K., Reddy, K.S., Schwartz, J. D., 2020. Exposure to particulate matter is associated with elevated blood pressure and incident hypertension in urban India. Hypertension 76 (4), 1289–1298.
Ramanathan, V., Carmichael, G., 2008. Global and regional climate changes due to black carbon. Nat. Geosci. 1, 221–227.
Rani, S.I., Ramachandran, R., Subrahamanyam, D.B., Alappattu, D.P., Kunhikrishnan, P. K., 2010. Characterization of sea/land breeze circulation along the west coast of Indian sub-continent during pre-monsoon season. Atmos. Res. 95 (4), 367–378.
Ravishankara, A.R., David, L.M., Pierce, J.R., Venkataraman, C., 2020. Outdoor air pollution in India is not only an urban problem. Proc. Natl. Acad. Sci. 117 (46), 28640.
Reddy, T.V.R., Mehta, S.K., Ananthavel, A., Ali, S., Annamalai, V., Rao, D.N., 2021. Seasonal characteristics of sea breeze and thermal internal boundary layer over Indian east coast region. Meteorog. Atmos. Phys. 133, 217–232.
Rimetz-Planchon, J., Perdrix, E., Sobanska, S., Brémard, C., 2008. PM_{10} air quality variations in an urbanized and industrialized harbor. Atmos. Environ. 42 (31), 7274–7283.
Rodríguez, S., Cuevas, E., González, Y., Ramos, R., Romero, P.M., Pérez, N., Querol, X., Alastuey, A., 2008. Influence of sea breeze circulation and road traffic emissions on the relationship between particle number, black carbon, PM1, PM2.5 and PM2.5–10 concentrations in a coastal city. Atmos. Environ. 42 (26), 6523–6534.
Sahu, S.K., Ohara, T., Beig, G., 2017. The role of coal technology in redefining India's climate change agents and other pollutants. Environ. Res. Lett. 12 (10), 105006.
Satheesh, S.K., Srinivasan, J., Moorthy, K.K., 2006. Spatial and temporal heterogeneity in aerosol properties and radiative forcing over Bay of Bengal: sources and role of aerosol transport. J. Geophys. Res. Atmos. 111, D8.
Singh, V., Singh, S., Biswal, A., 2021. Exceedances and trends of particulate matter ($PM_{2.5}$) in five Indian megacities. Sci. Total Environ. 750, 141461.
Srivastava, A.K., Singh, S., Tiwari, S., Kanawade, V.P., Bisht, D.S., 2012. Variation between near-surface and columnar aerosol characteristics during the winter and summer at Delhi in the Indo-Gangetic Basin. J. Atmos. Sol. Terr. Phys. 77, 57–66.
Stein, A.F., Draxler, R.R., Rolph, G.D., Stunder, B.J.B., Cohen, M.D., Ngan, F., 2015. NOAA's HYSPLIT atmospheric transport and dispersion modeling system. Bull. Am. Meteorol. Soc. 96, 2059–2077.
Stull, R., 1988. An Introduction to Boundary Layer Meteorology. Springer, Dordrecht.
Sumesh, R.K., Rajeevan, K., Resmi, E.A., Unnikrishnan, C.K., 2017. Particulate matter concentrations in the southern tip of India: temporal variation, meteorological influences, and source identification. Earth Syst. Environ. 1, 13.
Tan, Q., Ge, B., Xu, X., Gan, L., Yang, W., Chen, X., Pan, X., Wang, W., Li, J., Wang, Z., 2022. Increasing impacts of the relative contributions of regional transport on air pollution in Beijing: observational evidence. Environ. Pollut. 292, Part B, 118407.
Thomas, A., Sarangi, C., Kanawade, V.P., 2019. Recent increase in winter hazy days over Central India and the Arabian Sea. Sci. Rep. 9, 17406.
Thomas, A., Kanawade, V.P., Sarangi, C., Srivastava, A.K., 2021. Effect of COVID-19 shutdown on aerosol direct radiative forcing over the Indo-Gangetic Plain outflow region of the Bay of Bengal. Sci. Total Environ. 782, 146918.
Tripathi, S.N., Tare, V., Chinnam, N., Srivastava, A.K., Dey, S., Agarwal, A., Kishore, S., Lal, R.B., Manar, M., Kanawade, V.P., Chauhan, S.S.S., Sharma, M., Reddy, R.R., Gopal, K.R., Narasimhulu, K., Reddy, L.S.S., Gupta, S., Lal, S., 2006. Measurements of atmospheric parameters during Indian space research organization geosphere biosphere programme land campaign II at a typical location in the ganga basin: 1. Physical and optical properties. J. Geophys. Res. Atmos. 111, D23.
Tsai, H.-H., Yuan, C.-S., Hung, C.-H., Lin, C., Lin, Y.-C., 2011. Influence of sea-land breezes on the tempospatial distribution of atmospheric aerosols over coastal region. J. Air Waste Manage. Assoc. 61 (4), 358–376.
Upadhyay, A., Dey, S., Chowdhury, S., Kumar, R., Goyal, P., 2020. Tradeoffs between air pollution mitigation and meteorological response in India. Sci. Rep. 10, 14796.
Vadrevu, K.P., Eaturu, A., Biswas, S., Lasko, K., Sahu, S., Garg, J.K., Justice, C., 2020. Spatial and temporal variations of air pollution over 41 cities of India during the COVID-19 lockdown period. Sci. Rep. 10, 16574.
Varaprasad, V., Kanawade, V.P., Narayana, A.C., 2021. Spatio-temporal variability of near-surface air pollutants at four distinct geographical locations in Andhra Pradesh state of India. Environ. Pollut. 268, Part B, 115899.
Verma, S.B.P., Pani, S.K., Bharath Kumar, D., Faruqi, A.R., Bhanja, S.N., Mandal, M., 2016. Aerosol extinction properties over coastal West Bengal Gangetic plain under inter-seasonal and sea breeze influenced transport processes. Atmos. Res. 167, 224–236.
Wang, Y.Q., Zhang, X.Y., Draxler, R.R., 2009. TrajStat: GIS-based software that uses various trajectory statistical analysis methods to identify potential sources from long-term air pollution measurement data. Environ. Model Softw. 24 (8), 938–939.
Wei, J., Tang, G., Zhu, X., Wang, L., Liu, Z., Cheng, M., Münkel, C., Li, X., Wang, Y., 2018. Thermal internal boundary layer and its effects on air pollutants during summer in a coastal city in North China. J. Environ. Sci. 70, 37–44.
Williams, M.A., Raj, K.N., Rajesh, A.N., Kumar, T.V.L., Rao, D.N., 2022. Identification of sea breeze onset and its effect on surface black carbon aerosols over a tropical coastal environment (12.81°N, 80.03°E) in India. Pure Appl. Geophys. 179, 2993–3003.
Winker, D.M., Vaughan, M.A., Omar, A., Hu, Y., Powell, K.A., Liu, Z., Hunt, W.H., Young, S.A., 2009. Overview of the CALIPSO mission and CALIOP data processing algorithms. J. Atmos. Ocean. Technol. 26 (11), 2310–2323.
Xiao, Y., Yang, J., Cui, L., Deng, J., Fu, P., Zhu, J., 2023. Weakened sea-land breeze in a coastal megacity driven by urbanization and ocean warming. Earth's. Future 11, e2022EF003341.